Towards the quantification of α-synuclein aggregates with digital seed amplification assays

Supporting Information

Table of Contents:

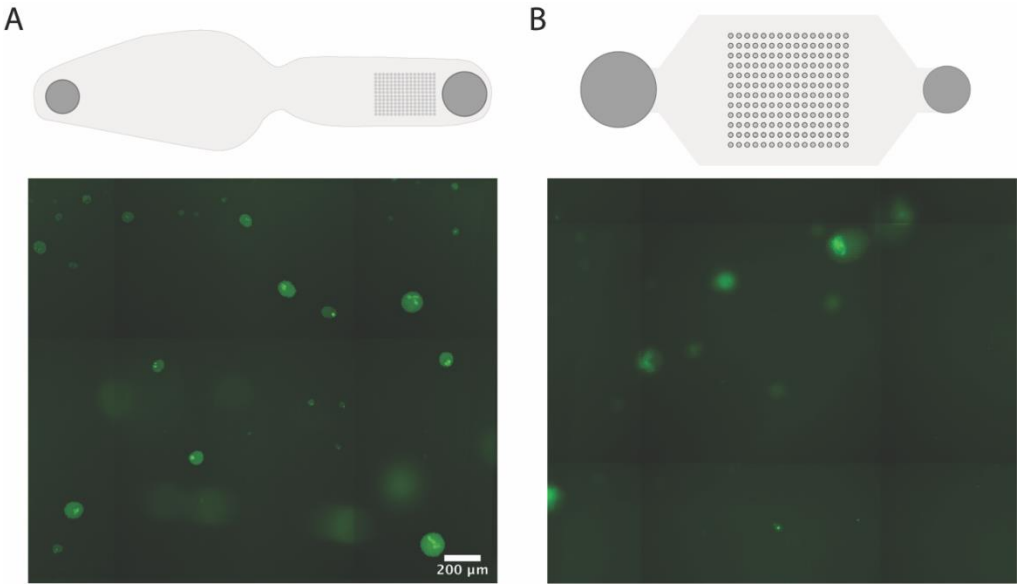

Figure S1. SAA in microwell arrays fabricated in cyclic olefin polymer (COP) and polydimethylsiloxane (PDMS). Fluorescence images of microwell arrays containing the SAA reaction including, PIPES pH 6.5, 100 mM NaCl, 0.1 mg/mL α-synuclein monomers, 5 ng/mL pre-formed α-synuclein filaments, and 10 µM ThT amyloid fibril staining dye. Both COP **(A)** and PDMS **(B)** based assays were not robust and could not be sealed properly.

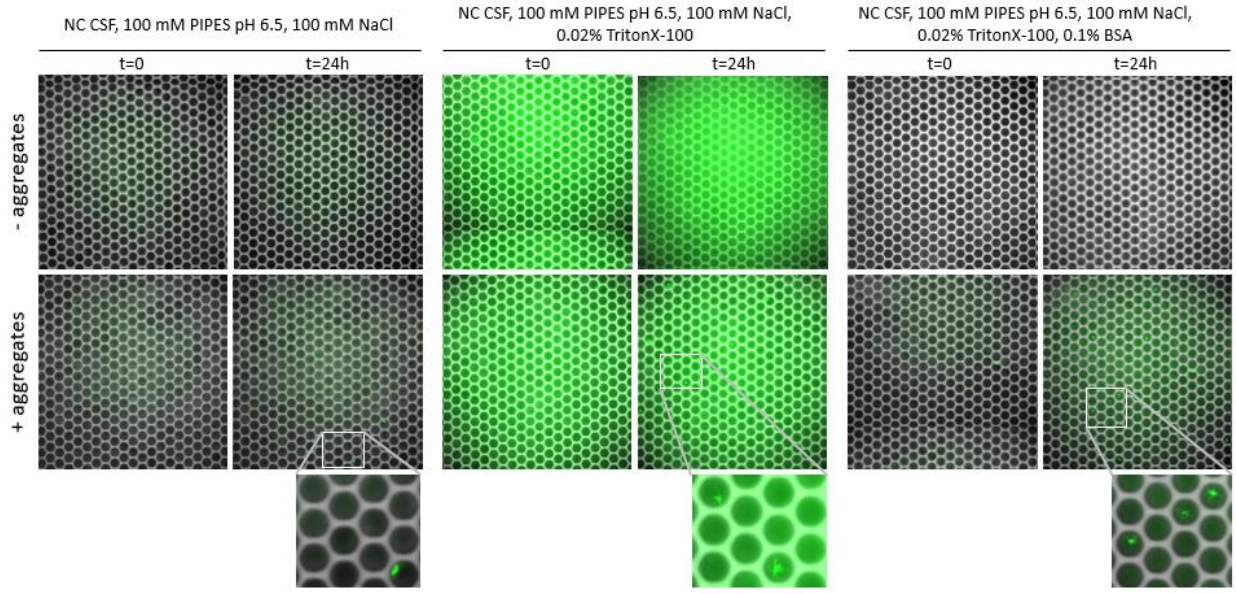

Figure S2. Microwell loading and surface blocking. (A) Using reaction conditions found to be optimal for bulk SAA reactions (100 mM 1,4-piperazinediethanesulfonic acid (PIPES) pH 6.5 and 100 mM NaCl), we could detect growing α-synuclein aggregates after 24 hours when 0.1 ng/ml pre-formed α-synuclein fibrils were spiked into the reaction solution (+aggregates); whereas we did not detect any aggregate growth in the negative control (- aggregates). Due to the seemingly hydrophobic nature of the SAA reaction mixture, we often saw incomplete microwell loading. **(B)** To increase the hydrophilicity of the SAA solution we added 0.02% Triton-X 100, which greatly improved microwell loading but led to a higher background signal, although we could still detect growing aggregates in the positive control and an absence of aggregates in the negative control (Inset). **(C)** Adding 0.1% bovine serum albumin (BSA) reduced non-specific binding to the surface and did not affect aggregate growth in the positive control or induce spontaneous aggregation in the negative control. All images shown depict approximately 400 microwells and are representative of the entire array.

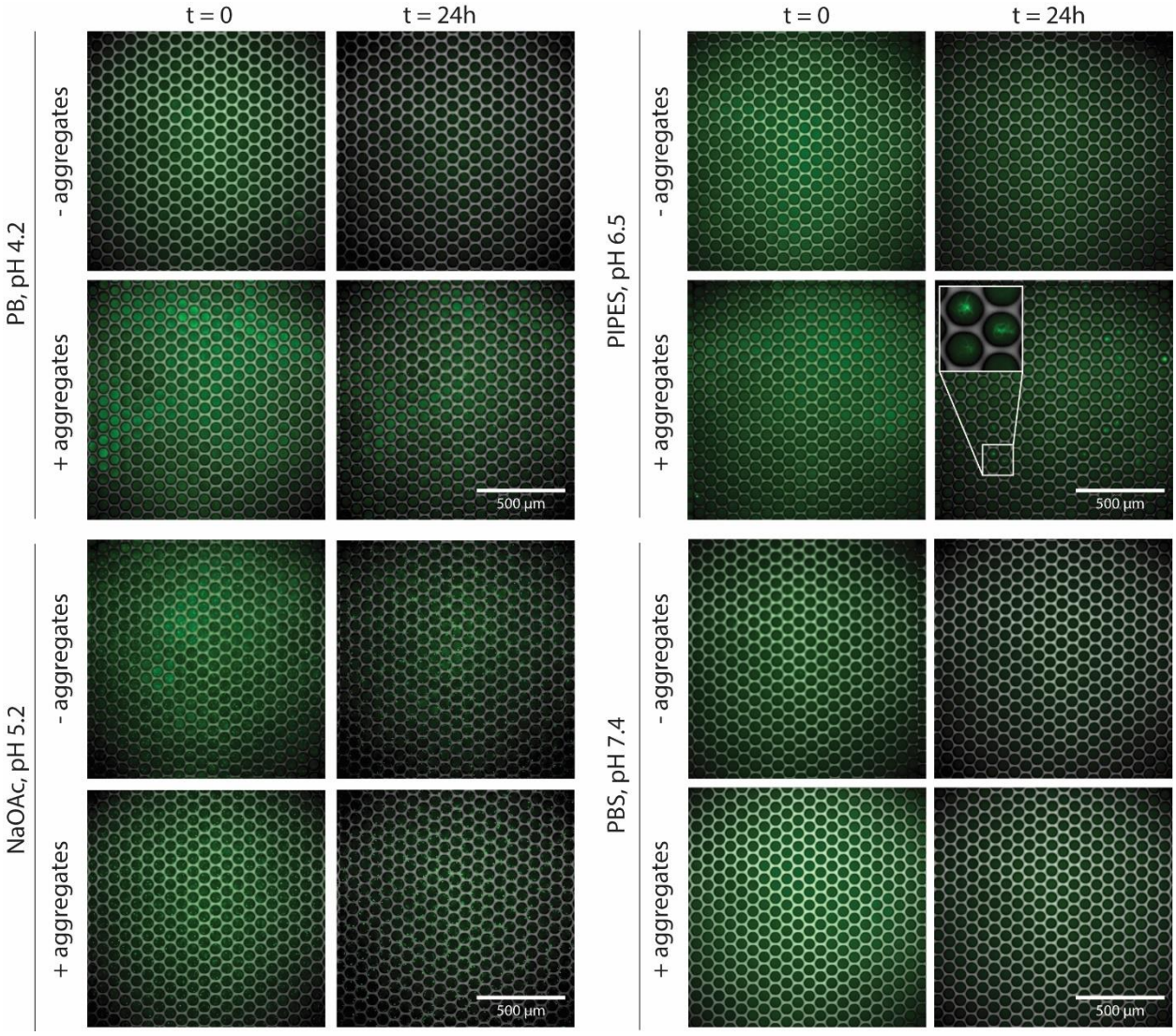

Figure S3. Optimizing buffer conditions in microwell arrays. Representative images of microwell arrays shown at times *t* = 0 and *t* = 24 hours for both negative (- aggregates) and positive (+aggregates) controls for four different buffer conditions: **(A)** potassium phosphate buffer (PB) pH 4.2, **(B)** sodium acetate buffer (NaOAc) pH 5.2, **(C)** PIPES buffer pH 6.5, and **(D)** phosphate buffered saline (PBS) pH 7.4. No aggregate growth was observed in PB or PBS in either the positive or negative control. Small aggregates grew in NaOAc, however they were not fibril-like and we saw similar globular structures growing at the edge of the wells in the negative control. PIPES buffer at a pH of 6.5 was the best condition, in which we observed aggregate growth in the positive control and no growth in the negative control.

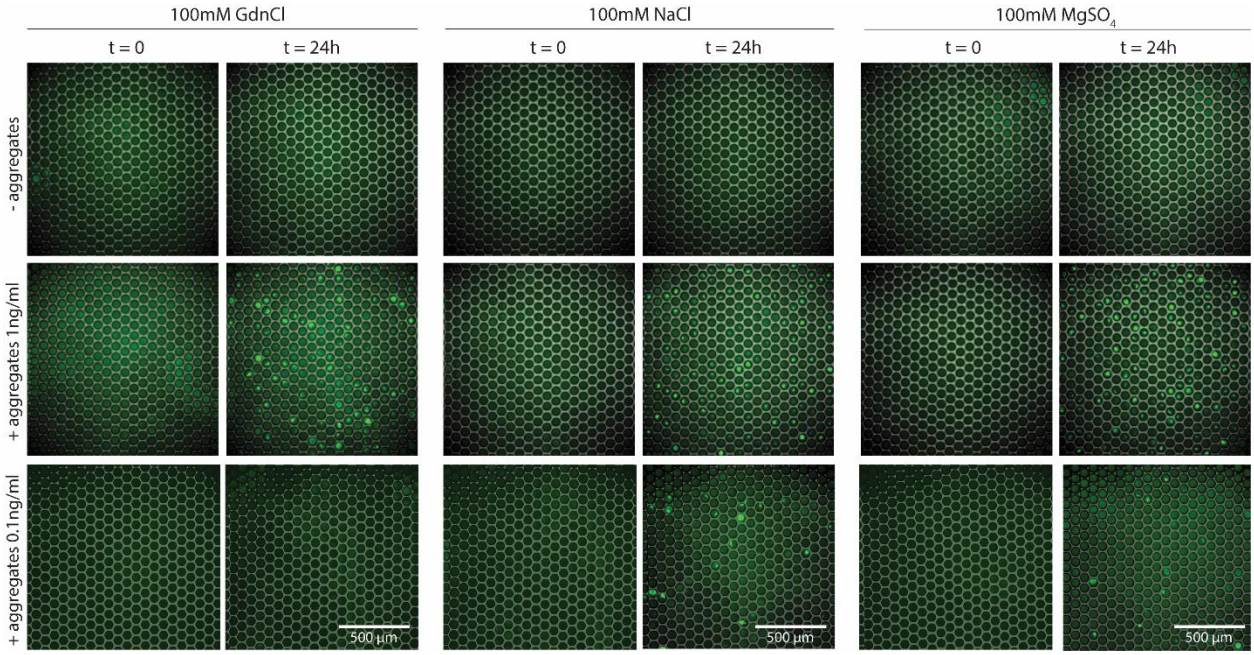

Figure S4. Adjusting lyotropic solution properties in microwells. Images of a subsection of the microwell array imaged at times *t* = 0 and *t* = 24 hours for the negative control (- aggregates) and two positive controls (+ aggregates) for pre-formed fibril spike-in concentrations of 1 ng/mL and 0.1 ng/mL. To strengthen and weaken hydrophobic interactions we tested three different salts: **(A)** guanidinium chloride (GdmCl), **(B)** sodium chloride (NaCl), and **(C)** magnesium sulfate ($MgSO_4$), each containing cations and anions that have varying effects on the solubility of proteins. In each case, 100 mM PIPES at a pH of 6.5, 0.02% Triton-X, and 0.1% BSA were also added. At a concentration of 1 ng/mL of pre-formed fibrils, we observed aggregate growth regardless of the salt added. However, at a lower concentration of 0.1 ng/mL, we observed optimal growth with NaCl.

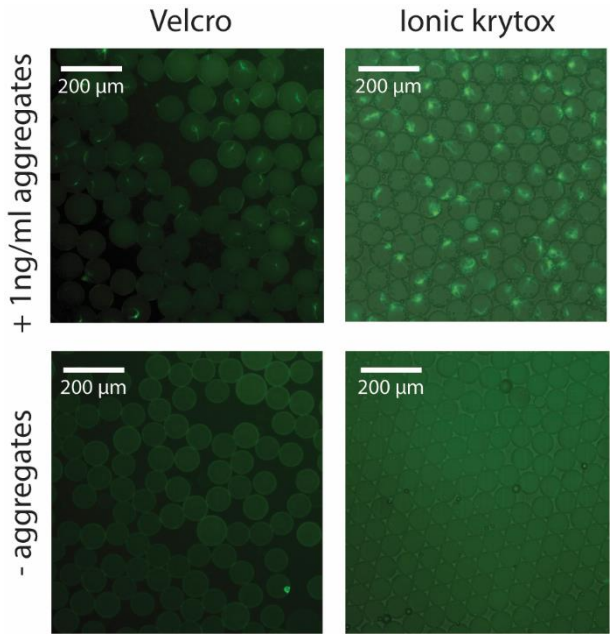

Figure S5. Digital SAA in droplets with Velcro and ionic krytox surfactants. Images of droplets containing SAA reaction mixtures including, PIPES pH 6.5, 100 mM NaCl, 0.1 mg/mL α-synuclein monomers, 5 ng/mL pre-formed α-synuclein filaments, and X-34 amyloid fibril staining dye. We encapsulated our SAA reaction mixtures in single emulsion droplets using a velcro and an ionic krytox surfactant. We were able to detect aggregates growing in both types of droplets when pre-formed fibrils were added (+ aggregates) and did not detect any growth in the negative controls (- aggregates).

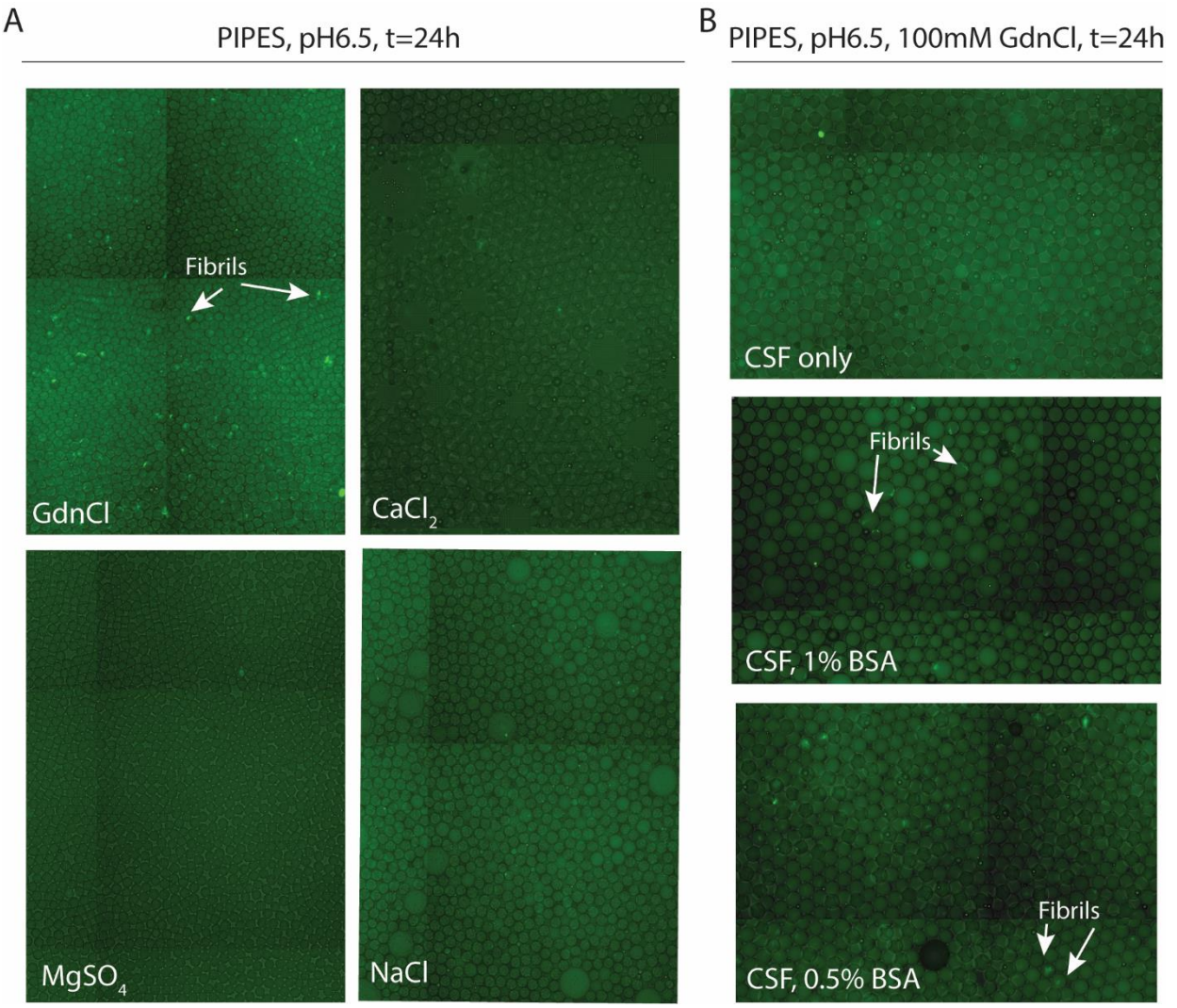

Figure S6. Optimizing SAA reaction conditions in droplets. (A) Based on our finding that PIPES buffer at a pH of 6.5 was ideal for aggregate growth in microwell arrays, we proceeded to screen different salts in droplets, including GdmCl, $MgSO_4$, $CaCl_2$, and NaCl, as shown in the representative images. In contrast to what we observed in the microwell arrays, in droplets we found GdmCl to be optimal for aggregate growth. **(B)** To prevent α-synuclein aggregates and monomers from non-specifically binding to the inner surface of the droplets, we added BSA into the reaction mixture. The condition when only CSF is added served as our control. We found that adding BSA at a concentration of 0.5% allowed us to see the greatest number of aggregates growing at a concentration of 1 ng/mL pre-formed fibrils. All droplets shown were generated with ionic krytox surfactant.

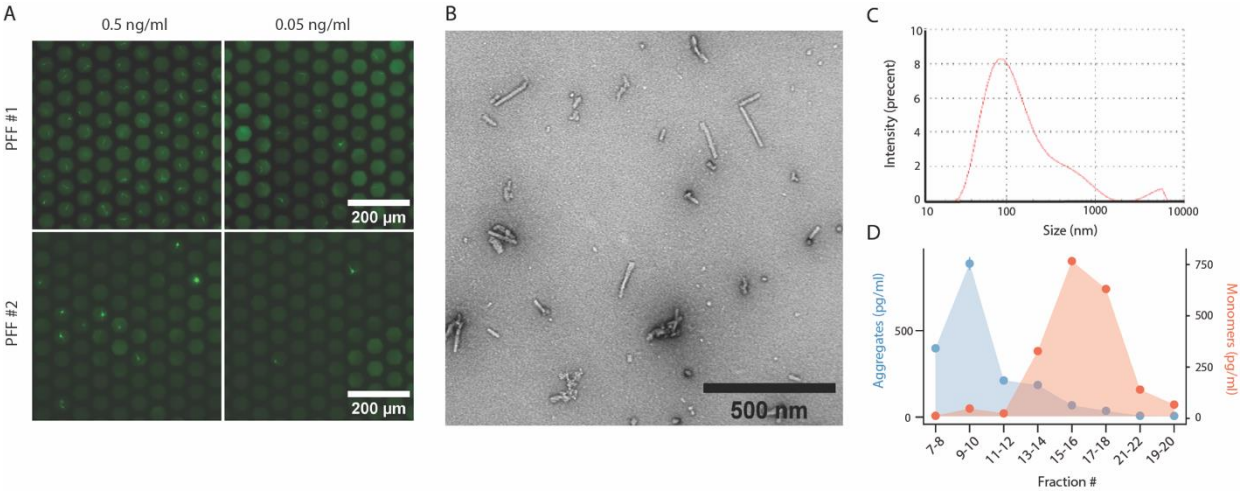

Figure S7. α-synuclein aggregate characterization. (A) Two batches of pre-formed α-synuclein fibrils (PFF #1 and PFF #2) were used as seeds in the microwell SAA and representative images are shown for two concentrations of pre-formed fibrils 24 h after running the amplification assay. The first batch of pre-formed fibrils was characterized using: **(B)** transmission electron microscopy (TEM), **(C)** dynamic light scattering, and **(D)** size exclusion chromatography (SEC) in combination with single-molecule array (Simoa) assays. The Simoa assays were performed according to Norman et al.[1]

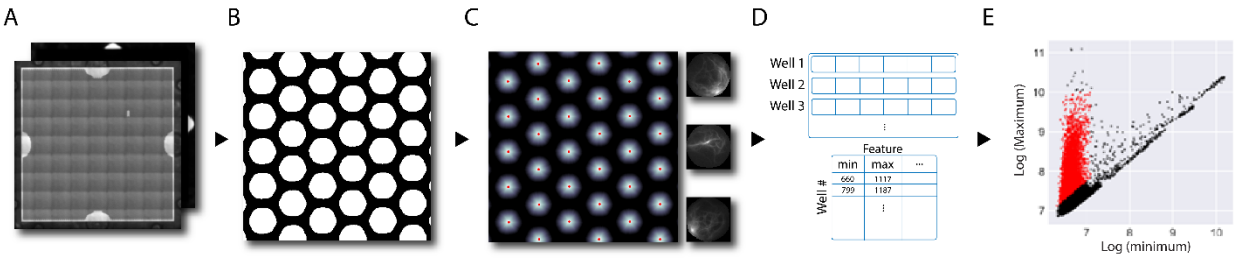

Figure S8. Image processing pipeline. Data extraction and image processing were performed using Python (3.10) and the scikit-image (0.19), numpy (1.23), and pandas (1.4) packages. The raw images contained two channels, a fluorescence channel and a brightfield channel **(A)**. The brightfield channel was binarized **(B)** and used to detect the center point of each well **(C, left)**. Then, each well was individually extracted from the fluorescence channel as a separate 90x90 pixel image **(C, right)**. Each image was reshaped to be a 1-dimensional vector with 8100 values. All images were then combined into a single matrix W of dimension (n_wells, 8100) **(D, top)** with n_wells ~13,000. W was then analyzed, and features were generated (such as well minimum or maximum, aggregate eccentricity, etc.) in a separate metadata matrix M with dimension (n_wells, n_features) **(D, bottom)**. These features were then used for initial well classification to create a model training set for a generalized classification model **(E)**.

pathology diagnosis	tissue	gender	age
PD	frontal cortex	F	87
PD	frontal cortex	M	73
MSA-P	frontal cortex	F	67
MSA-P	frontal cortex	F	61
NC	frontal cortex	M	62
NC	frontal cortex	M	56
MSA-C	CSF	F	63
MSA-C	CSF	F	48
PD	CSF	M	70
PD	CSF	M	69
NC	CSF	M	67
NC	CSF	M	72

Table S1 Characteristics of the clinical samples. Sample types collected from PD and MSA patients and NCs, including the sex and age of each individual.

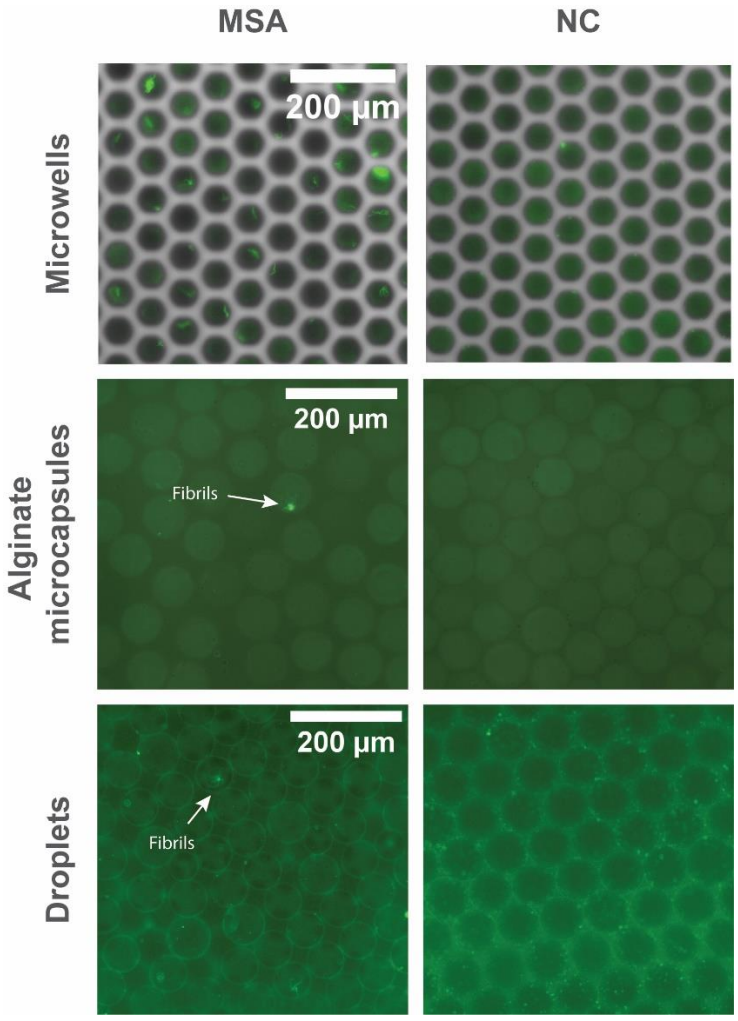

Figure S9: Assay validation using human brain lysates. Images of microwells, alginate microcapsules, and droplets containing the optimized SAA reaction mixtures with 100X dilution of MSA and NC human brain lysates. Growing aggregates were detected in the MSA samples using all three platforms.

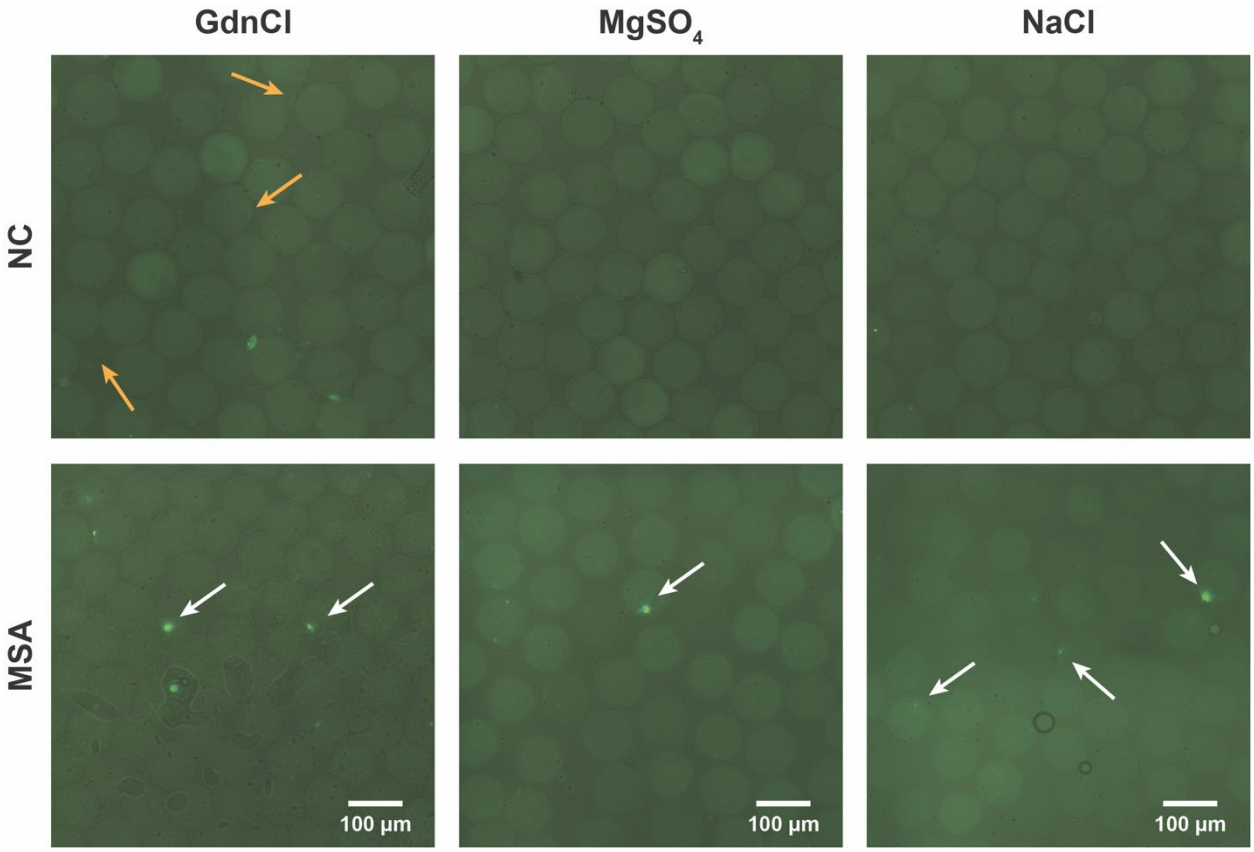

Figure S10. Optimizing SAA reaction conditions for clinical samples in alginate microcapsules. NC and MSA brain lysates were analyzed with the hydrogel microcapsule SAA using PIPES buffer and three different salts: GdnCl, $MgSO_4$, and NaCl. Representative images acquired after running the SAA reaction for 24 h are shown. White arrows indicate growing fibrils in the MSA samples and orange arrows indicate small false positive fibrils seen in the NC sample when GdnCl was used.

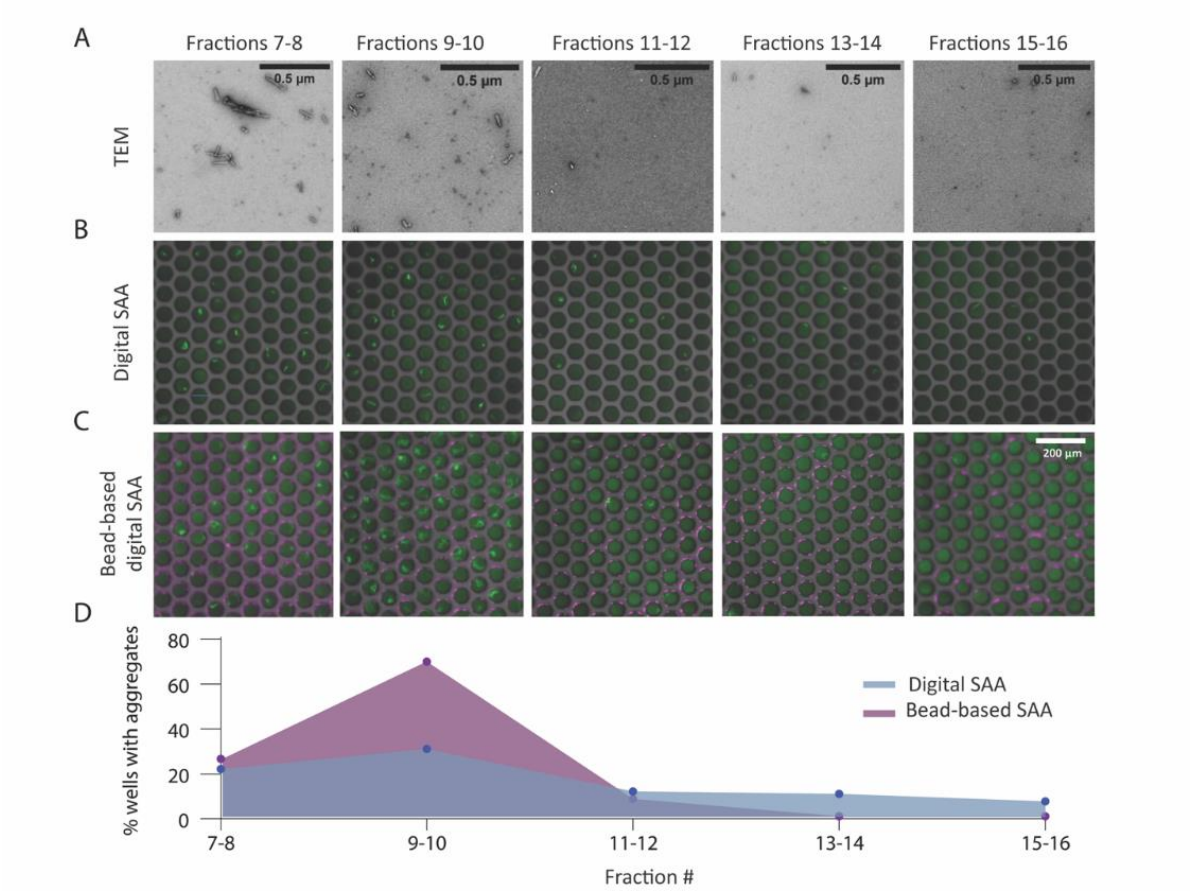

Figure S11. Analysis of pre-formed filaments by TEM, SAA, and SEC. Pre-formed filaments were separated by size using SEC. Fractions 7-8, 9-10, 11-12, 13-14, and 15-16 were imaged with TEM **(A)** and used as seeds for the standard digital SAA **(B)** and the bead-based digital SAA **(C)**. In each case, representative TEM or microwell images are shown. **(D)** The percent of wells detected with growing aggregates versus the SEC fraction for both the standard digital SAA and the bead-based SAA.

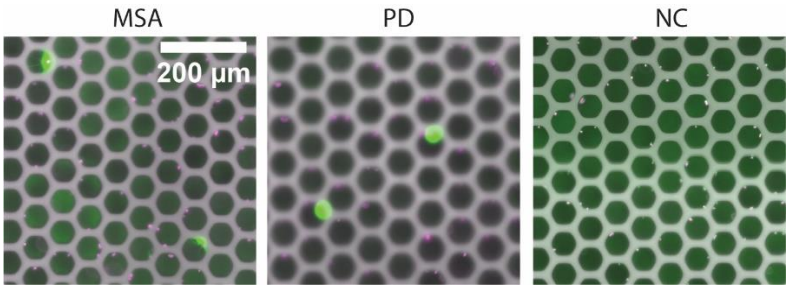

Figure S12: Analysis of human brain lysates with the bead-based digital SAA. Representative images after 48 h of running the amplification assays with beads that were incubated in a 40X dilution of MSA, PD, and NC brain lysates.

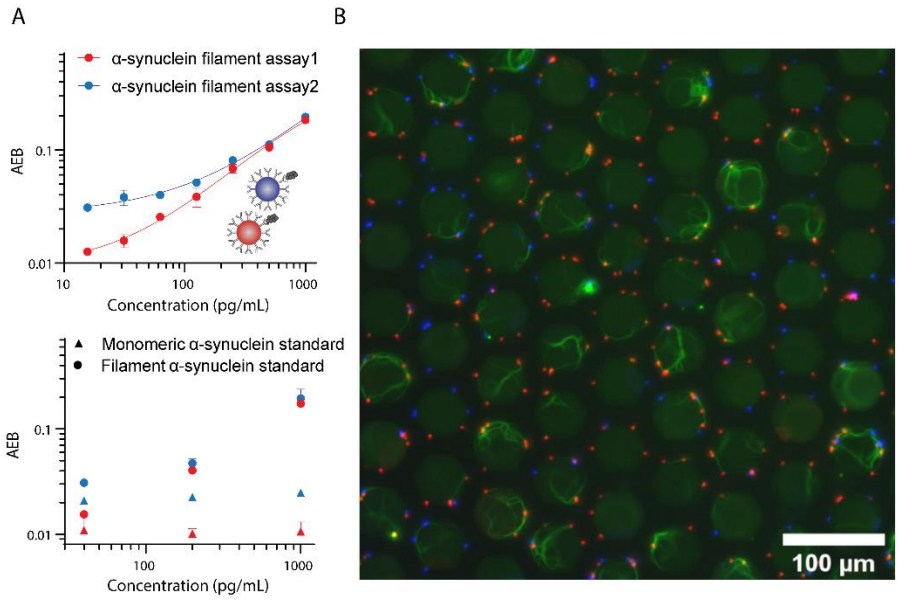

Figure S13. Multiplexed bead-based digital SAA. (A) Top—the Simoa assay calibration curve for two different antibody-coated magnetic capture beads, Syn-F1 (red) and Syn7015 (blue). Bottom—each assay is run using either monomeric or filamentous α-synuclein as the protein standard, demonstrating each antibody's specificity toward α-synuclein filaments. **(B)** Representative image of the multiplexed bead-based SAA where beads coated with either Syn-F1 (red) or Syn7015 (blue) antibodies were used to pre-capture aggregates. Single α-synuclein filaments were observed to grow from both colored beads.

References

1. Norman M, Gilboa T, Walt DR. High-Sensitivity Single Molecule Array Assays for Pathological Isoforms in Parkinson's Disease. *Clin Chem*. Published online January 22, 2022:hvab251. doi:10.1093/clinchem/hvab251